1,3-Dialkyltriazenyl Radicals: Their Electron Spin Resonance Spectra, Electronic Configuration, and Addition to Trialkyl Phosphites

John C. Brand and Brian P. Roberts *

Christopher Ingold Laboratories, University College London, 20 Gordon Street, London WC1H 0AJ

The 1,3-dialkyltriazenyl radicals $\overline{RN\dot{N}NR}$, in which R = CH_3, CD_3, Pr^i, or Bu^t, have been generated in solution from the parent triazenes and studied by e.s.r. spectroscopy. The triazenyl radicals exhibit large hyperfine splitting from the central nitrogen, smaller splitting from two equivalent alkylated nitrogens, and characteristically low *g* factors of *ca.* 2.0020. These spectroscopic parameters are as expected for a σ-radical, in which the SOMO is in the NNN plane, and this electronic configuration is supported by the results of semiempirical molecular orbital calculations. Dialkyltriazenyl radicals add to trialkyl phosphites to give the cyclic triazyl radicals (*A*), which may be regarded as 'spin-labelled' phosphoranes. The same

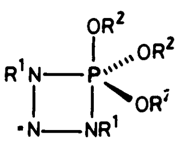

(*A*)

radicals are produced by cyclisation of dialkyltriazeno(trialkoxy)phosphoranyl radicals $(R^2O)_3\dot{P}N(R^1)N{=}NR^1$. The e.s.r. spectra of the spin-labelled phosphoranes exhibit temperature-dependent lineshape effects which are attributed to exchange of apical and equatorial nitrogen ligands, and an activation energy of 22 kJ mol^{-1} for this exchange was obtained by computer simulation of the spectra for (*A*; R^1 = Bu^t, R^2 = Me).

The allyl radical ($H_2C{=}CH{-}\dot{C}H_2$), nitrogen dioxide ($O{=}N{-}\dot{O}$), and the triazenyl radical ($HN{=}N{-}\dot{N}H$) are members of a family of radicals which each contain 17 valence electrons and in which the unpaired electron is delocalised over three heavy atoms from the first row of the Periodic Table. For any member, provided that all atoms are coplanar, σ- and π-orbitals may be distinguished and the unpaired electron could, in principle, occupy either type of orbital. The SOMO of the allyl radical is a non-bonding π-orbital that has a nodal plane containing the central C-H group. Allyl is thus a π-radical in which all 14 σ-electrons are involved in bonding, and the σ-radical configuration will be an excited state of much higher energy.

However, for isoelectronic species containing fewer σ-bonds than allyl, σ-radical ground states become energetically feasible. Thus, it is well established that nitrogen dioxide is a σ-radical[1] in which the unpaired electron occupies an in-plane three-centre molecular orbital and is strongly associated with the central nitrogen atom.

Molecular orbital calculations predict that triazenyl is also a σ-radical, but that this electronic state is only 6.7 kJ mol^{-1} more stable than the π-configuration.[2] However, in 1978 Lunazzi and his co-workers[3] reported the generation of the 1,3-dimethyltriazenyl radical, by hydrogen abstraction from the parent triazene and concluded, on the basis of the magnitudes of the coupling constants obtained by analysis of its e.s.r. spectrum, that this species is a π-radical. In a preliminary communication[4] we have reported that this e.s.r. spectrum was incorrectly interpreted by Lunazzi *et al.* and that the correct coupling constants are as expected for a σ-radical. In the present paper we give a full account of our e.s.r. studies of 1,3-dialkyltriazenyl radicals, including an investigation of their addition reactions with trialkyl phosphites.[5]

$$Bu^tOOBu^t \xrightarrow{h\nu} 2Bu^tO\bullet \qquad \text{(i)}$$

$$Bu^tO\bullet + RN(H)N{=}NR \longrightarrow \overset{\bullet}{\overline{RN^1N^2N^3R}} + Bu^tOH \qquad \text{(ii)}$$

(1)

$$Bu^tON{=}NOBu^t \longrightarrow 2Bu^tO\bullet + N_2 \qquad \text{(iii)}$$

Results

U.v. photolysis of cyclopropane † solutions containing di-t-butyl peroxide (DTBP) (15—20% v/v) and a 1,3-dialkyltriazene (7—15% v/v), while the sample was in the cavity of the e.s.r. spectrometer,[6] gave rise to a spectrum which we ascribe to the 1,3-dialkyltriazenyl radical (1) [equations (i) and (ii)]. The e.s.r. parameters for (1; R = Me, Pr^i, or Bu^t) are given in Table 1 and the spectra of (1; R = Me) and (1; R = Pr^i) are shown in Figures 1 and 2, respectively. The spectrum of (1; R = Bu^t) is given in ref. 4. Since our analysis of the spectrum of (1; R = Me) differs in a crucial way from that given by Lunazzi *et al.*,[3] we also generated the fully deuteriated analogue (1; R = CD_3). The spectrum of (1; R = CD_3) (see Table 1) confirmed our analysis of that of the unlabelled radical.

The dialkyltriazenyl radicals were short lived and their spectra disappeared within the fall time of the instrument (0.3 s) when photochemical generation was interrupted. The di-t-butyltriazenyl radical (1; R = Bu^t), but not (1; R = Me), could also be detected during thermolysis of di-t-butyl

---

† Dimethyltriazene was not very soluble in cyclopropane at very low temperatures and benzene, dichloromethane, or diethyl ether were present as co-solvents in some experiments.

Table 1. E.s.r. parameters for 1,3-dialkyltriazenyl radicals in cyclopropane

Radical	T/K	g-Factor	Hyperfine splittings (G) $a(\mathrm{N}^{\mathrm{central}})$	 a(2N)	 a(H) [a]
$\mathrm{Me}\overline{\mathrm{N}\dot{\mathrm{N}}\mathrm{N}}\mathrm{Me}$	226	2.0021	11.5	4.0	8.0 (6)
$\mathrm{CD_3}\overline{\mathrm{N}\dot{\mathrm{N}}\mathrm{N}}\mathrm{CD_3}$	225	2.0021	11.5	4.0	1.2 (6) [b]
$\mathrm{Pr^i}\overline{\mathrm{N}\dot{\mathrm{N}}\mathrm{N}}\mathrm{Pr^i}$	222	2.0020	12.2 [c]	3.5 [d]	5.1 (2) [e]
$\mathrm{Bu^t}\overline{\mathrm{N}\dot{\mathrm{N}}\mathrm{N}}\mathrm{Bu^t}$	229	2.0019	12.3 [c]	3.1 [f]	
$\mathrm{Me}\overline{\mathrm{N}\dot{\mathrm{N}}\mathrm{N}}\mathrm{SiMe_3}$	181	2.0011	16.8	[g]	
$\mathrm{Me_3Si}\overline{\mathrm{N}\dot{\mathrm{N}}\mathrm{N}}\mathrm{SiMe_3}$ [h]	285	2.0002	20.6	[i]	
$\overline{\mathrm{O}\dot{\mathrm{N}}\mathrm{O}}$ [j]	110	2.0000	54.3		

[a] Number of equivalent nuclei shown in parentheses. [b] Deuterium splitting. [c] Essentially independent of temperature. [d] $\mathrm{d}|a(2\mathrm{N})|/\mathrm{d}T = +3$ mG K^{-1}. [e] $\mathrm{d}|a(2\mathrm{H})|/\mathrm{d}T = +5$ mG K^{-1}. [f] $\mathrm{d}|a(2\mathrm{N})|/\mathrm{d}T = +2$ mG K^{-1}. [g] Non-equivalent nitrogens: a(1N) 3.4, a(1N) 1.8 G (compare ref. 8). [h] Data from ref. 8. [i] Not resolved. [j] Data from J. R. Morton, K. F. Preston, and S. J. Strach, *J. Phys. Chem.*, 1979, **83**, 533.

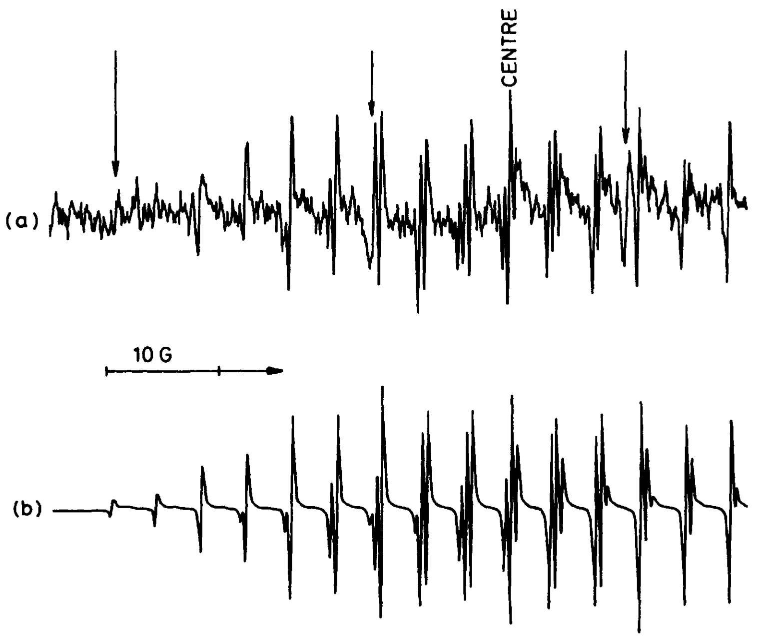

Figure 1. (a) Part of the e.s.r. spectrum of the 1,3-dimethyltriazenyl radical obtained during photolysis of a cyclopropane solution containing 1,3-dimethyltriazene (7% v/v) and di-t-butyl peroxide (20% v/v) at 221 K. The arrows indicate the first three lines in the spectrum of the methyl radical (see text). (b) Computer simulation of the spectrum of the 1,3-dimethyltriazenyl radical using the parameters given in Table 1

hyponitrite [7] in the presence of the parent triazene at 335 K in benzene [equation (iii) followed by (ii)].

The e.s.r. spectra of (1) are characterised by a large splitting from the central nitrogen and smaller splitting from the two terminal nitrogens; proton splittings originating from magnetically equivalent N-alkyl groups were detected for (1; R = Me or $\mathrm{Pr^i}$). The g-factors are less than the free-spin value (2.0023). The spectra of (1) are similar to those of the 1,3-disubstituted triazenyl radicals formed by addition of trialkylsilyl radicals to alkyl azides [*e.g.*, equation (iv)],[8] and the spectroscopic parameters of (2) are included in Table 1. Further confirmation that addition of trialkylsilyl radicals takes place at the terminal nitrogen of the alkyl azide to give (2),[8] rather than at the alkylated nitrogen to give $\mathrm{Me_3Si(Me)NN{=}N^{\bullet}}$, was obtained from experiments with $\mathrm{Me_3Si(Me)NN{=}NMe}$.[9] Photolysis of this silylated triazene at 206 K gives $\mathrm{N_2}$, $\mathrm{Me_3Si(Me)N^{\bullet}}$, and $\mathrm{Me^{\bullet}}$, and the spectrum ascribed to (2) is not detected. Thus, it appears that $\mathrm{Me_3Si(Me)NN{=}N^{\bullet}}$, unlike (2), is very unstable with respect to loss of nitrogen.

In photolytic experiments, most of the u.v. light incident on the sample is in the waveband *ca.* 260—340 nm [10] and the dialkyltriazenes absorb strongly in this region.* In fact, they absorb much more strongly than DTBP and it is possible that energy transfer [11] from excited triazene to DTBP may be involved in the formation of t-butoxyl radicals from the latter.

Photolysis of the triazenes alone in cyclopropane also afforded e.s.r. spectra of the appropriate triazenyl radicals, although these spectra were much stronger in the presence of DTBP. A gas, presumably nitrogen, was evolved in the presence or absence of DTBP. In addition to the spectrum of (1; R = Me), a weak spectrum of the methyl radical (indicated in Figure 1) was also detected during photolysis of dimethyltriazene, with or without DTBP, and $\mathrm{Me^{\bullet}}$ presumably arises from the cleavage shown in equation (v). The origin of (1) in the absence of DTBP is less clear. Direct cleavage of the N–H bond is possible, as is abstraction of hydrogen from ground-state triazene by photoexcited triazene or by the alkylaminyl radical.

---

* U.v. spectra were recorded, using a Perkin-Elmer 554 instrument, in iso-octane under nitrogen at room temperature. The dialkyltriazenes RN(H)N=NR showed [R, $\lambda_{\mathrm{max.}}$(ε/ l $\mathrm{mol^{-1}\ cm^{-1}}$), $\varepsilon_{280\mathrm{nm}}$/l $\mathrm{mol^{-1}\ cm^{-1}}$]: Me, 224 nm ($2.8 \times 10^3$), 2.0×10^2; $\mathrm{Pr^i}$, 234 nm (9.3×10^3), 4.2×10^2; $\mathrm{Bu^t}$, 238 nm (8.0×10^3), 3.2×10^2. For comparison, DTBP shows ε_{280} 4.2 l $\mathrm{mol^{-1}\ cm^{-1}}$, in agreement with the value reported previously (E. R. Bell, F. F. Rust, and W. E. Vaughan, *J. Am. Chem. Soc.*, 1950, **72**, 337), but this compound exhibits a well defined absorption maximum at 242 nm (ε_{242} 8.3, ε_{220} 3.0 l $\mathrm{mol^{-1}\ cm^{-1}}$) and not continuously increasing structureless absorption down to 220 nm, as reported by Bell *et al.*

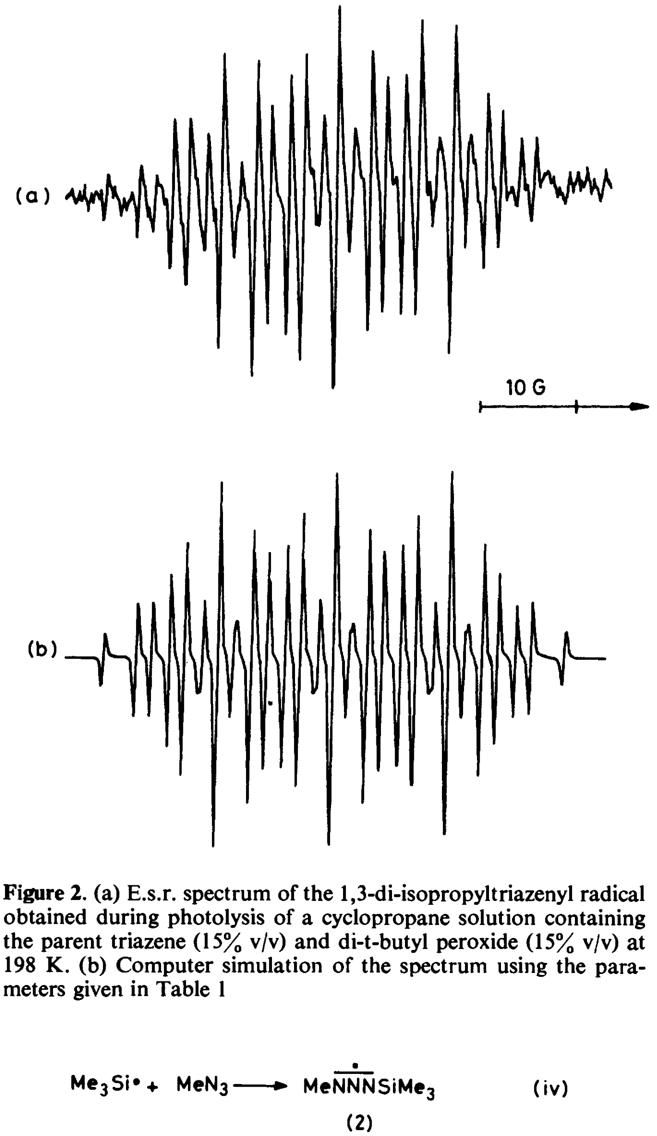

Figure 2. (a) E.s.r. spectrum of the 1,3-di-isopropyltriazenyl radical obtained during photolysis of a cyclopropane solution containing the parent triazene (15% v/v) and di-t-butyl peroxide (15% v/v) at 198 K. (b) Computer simulation of the spectrum using the parameters given in Table 1

$$Me_3Si\cdot + MeN_3 \longrightarrow Me\overline{N\dot{N}N}SiMe_3 \qquad \text{(iv)}$$

(2)

$$MeN(H)N{=}NMe \xrightarrow{h\nu} Me\dot{N}H + N_2 + Me\cdot \qquad \text{(v)}$$

Formation of the methylaminyl radical [equation (v)] during photolysis of dimethyltriazene was confirmed by carrying out the experiment in the presence of triethyl phosphite (*ca.* 1M) at 165 K in cyclopropane–diethyl ether solvent. Spectra assignable [12] to the two phosphoranyl adducts (3) and (4) were detected * along with the spectrum of the 'spin-labelled' phosphorane (5) (see below), produced by trapping of $Me\dot{N}H$, Me·, and (1; R = Me), respectively. No spectrum attributable to the phosphoranyl radical analogous to (3), which would be formed by the trapping of $Bu^t\dot{N}H$, could be detected during photolysis of di-t-butyltriazene with trimethyl phosphite in ethylene solvent at 143 K.

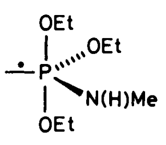

(3)

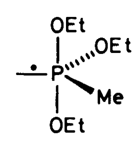

(4)

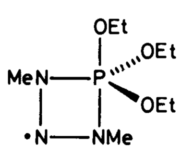

(5)

Molecular Orbital Calculations.—The dimethyltriazenyl radical was also investigated using semiempirical molecular orbital calculations. Preliminary MINDO/3-UHF calculations [13] with full structural optimisation from starting geometries in which $\widehat{NNN}$ was 120° were attempted, but led to energy minima for which this angle was close to 180°. This linear arrangement appears implausible and it is known that the MINDO/3 method overestimates the central angle in related radicals. Thus, the calculated value for $\widehat{ONO}$ in nitrogen dioxide is 153.7°, 19.4° greater than the experimentally determined value of 134.3°.[13] In subsequent calculations, $\widehat{NNN}$ was fixed at 134°, a choice which can be justified in the following way.

Ab initio calculations (STO-3G + CI) for planar $H\overline{N\dot{N}N}H$ gave $\widehat{NNN}$ 126°.[2] Similar calculations for the isoelectronic nitrogen dioxide gave $\widehat{ONO}$ 126° also, but at the 4-31G + CI level the angle increased to 134°, equal to the experimentally determined value.[2] Hence, it appears reasonable to assume that $\widehat{NNN}$ in $H\overline{N\dot{N}N}H$ would also increase towards a more correct value at the 4-31G + CI level and that a reasonable optimum value will be *ca.* 134°.

In all MINDO/3-UHF calculations the C–H bond lengths were fixed at 1.09 Å and all HCN angles were fixed at 110°. The N–N and C–N lengths and CNN angles were optimised, within the constraint that the two N–N distances were kept equal. For structures in which the CNNNC system was planar, three minima were located and these are shown in (6)—(8). The conformation about the C–N bond is such that a C–H bond is antiperiplanar to an N–N bond, but it was shown that rotation about the C–N bond was, as expected, a very low energy process (barrier 1—3 kJ mol^{-1}).

The structures (6)—(8) were local minima with respect to movement of the carbon atoms out of the NNN plane. Local minima could also be found from starting geometries in which one or both C–N bonds were at 90° to the NNN plane, but these structures were all less stable than (7), although the energy differences were small.

Starting with $\widehat{NNN}$ 60° and with the methyl groups on opposite sides of the NNN plane, a local minimum corresponding to the triazacyclopropyl radical (9) was found. The unpaired electron is contained in a π-type orbital and primarily associated with the unique nitrogen. However, (9) was much less stable than (6)—(8), as expected in view of previous calculations which predict triazacyclopropane $H\overline{NNHN}H$ to be much less stable than the acyclic triazene $H_2N{-}N{=}NH$.[14] It is thus unreasonable that triazacyclopropyl radicals should be formed from acyclic precursors, in particular from dialkyltriazenes by hydrogen abstraction or from azides by addition of trialkylsilyl radicals.[15]

INDO I (K = 1) calculations [15] were also carried out for the optimised structures (6)—(8) and the predicted nitrogen hyperfine splittings (in gauss) and total energies (in eV) are given in (6a)—(8a). These calculations predict that stability decreases in the order (6) > (7) > (8), whilst the MINDO/3 calculations predict the order (7) > (6) > (8). However, only for (6) are the predicted nitrogen splittings in reasonable accord with experiment, and it appears that terminal nitrogens with attached *endo*-methyl groups would give rise to large hyperfine splittings. Of course, for structure (7) to be consistent with the experimental results, *exo-endo* methyl exchange would have to be rapid on the e.s.r. time scale at all temperatures studied.

---

* For (3), *a*(P) 858.0, *a*(N) 3.0 G and *g* 2.0020, and for (4), *a*(P) 791.2 G and *g* 2.0021 at 165 K.

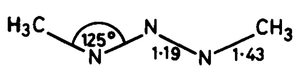

(6)

Total energy(eV) -919·078

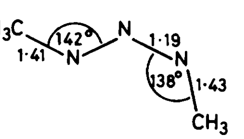

(7)

-919·431

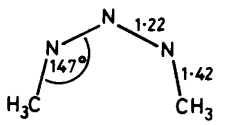

(8)

-918·943

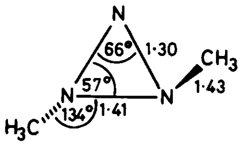

(9)

-917·742

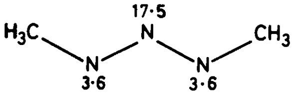

(6a)

-1406·284

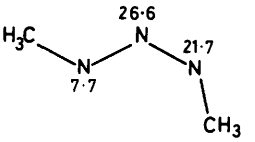

(7a)

-1406·110

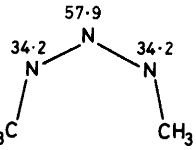

(8a)

-1405·687

The unpaired electrons in (6)—(8) are contained in σ-orbitals in the CNNNC plane. We conclude that the 1,3-dimethyltriazenyl radical adopts the planar (*E,E*)-configuration (6) and that it is a σ-radical.

Proton Splittings.—INDO calculations were also used to probe the angular dependence of the methyl proton splittings for the configuration (6) and these results are given in (10a—c) [splittings (in gauss) and relative energies (in kJ mol^{-1}) are shown]. Of these, (10a) was the most stable. However, the mean proton splittings for (10a—c) range from 2.2—2.5 G, in poor agreement with the experimental value of 8.0 G.

Reaction of Dialkyltriazenyl Radicals with Trialkyl Phosphites.—The spectrum of (1), obtained when the parent triazene was photolysed alone, was strongest from 1,3-di-t-butyltriazene. However, when trimethyl phosphite was also present at 205 K, the spectrum of (1; R = Bu^t) was quenched and replaced by that shown in Figure 3. This spectrum can be analysed in terms of splitting from ^{31}P and two non-equivalent ^{14}N nuclei (see Table 2) and it is assigned to the triazyl radical (11; R = Me), which may also be regarded as a ' spin-labelled ' phosphorane (SLP). The larger nitrogen splitting (13.0 G) is assigned to N^2 and the smaller splitting (2.6 G) to the apical nitrogen [N^3 in (11a)], rather than to the equatorial nitrogen, because the canonical structure (12a) would be expected to make a larger contribution than (12b) since, in trigonal-bipyramidal phosphoranes, electronegative ligands preferentially occupy apical sites and π-electron donors prefer equatorial locations.[16]

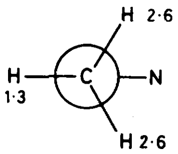

(10a)

0·0

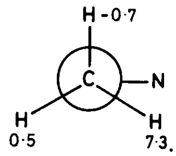

(10b)

+1·1

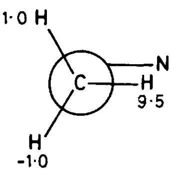

(10c)

+1·6

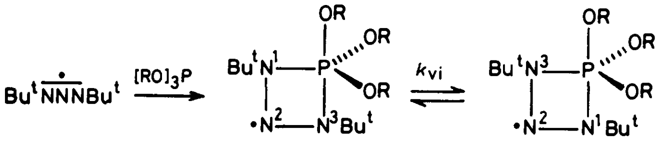

(11a) (11b) (vi)

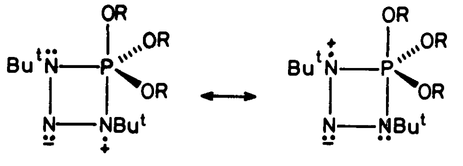

(12a) (12b)

Table 2. E.s.r. parameters for spin-labelled phosphoranes in cyclopropane

Radical [a]	*T*/K	*g*-Factor	Hyperfine splittings (G) *a*(P) [b]	*a*(N^2)	Others [c]
(5)	219	2.0033	11.3	13.1	1.9 (2N), 1.9 (6H)
	255		12.5	13.2	1.9 (2N), 1.9 (6H)
(11; R = Me)	205	2.0034	7.3	13.0	2.6 (1N)
	282		12.3	13.0	1.4 (2N)
(11; R = Et)	218	2.0036	7.5	13.0	3.0 (1N)
	295		12.3	13.0	1.5 (2N)
(11; R = Pe^{neo})	204	2.0034	5.4	13.1	3.1 (1N)
	235		6.8	13.1	3.1 (1N)
(13; R = Bu^t)	222	2.0034	7.7	13.0	1.7 (2N)
	263		9.6	13.0	1.7 (2N)
(13; R = Pe^{neo})	231	2.0034	8.1	13.0	1.4 (2N)
	280		11.5	13.0	1.5 (2N)

[a] The radical (5) was highly transient, but (11) and (13), which have bulky *N*-t-butyl groups, were longer lived. For example, approximate first half-lives for (11; R = Me) were 45 s at 249 K and 5 s at 273 K; for (11; R = Pe^{neo}) at 249 K, the first half-life was 6 s. Decay of these SLPs may take place by way of fragmentation to the shorter lived di-t-butyltriazenyl radical. [b] The phosphorus splittings increased linearly with temperature over the ranges investigated [c] Numbers of equivalent nuclei shown in parentheses.

Inspection of Figure 3 shows that the appearance of the spectrum is highly temperature dependent. As the temperature increases, the phosphorus splitting increases markedly, new lines appear, and lineshape changes are evident. We interpret the latter two effects in terms of rapid exchange of N^1 with N^3, as a result of interconversion of (11a and b) [equation (iv)]. At any given temperature the appearance of the spectrum was independent of the concentrations of triazene (0.5—1.6M) or phosphite (0.7—2.0M), confirming that the exchange is intramolecular. Above *ca.* 280 K when R = Me, interconversion of (11a and b) takes place sufficiently rapidly to render N^1 and N^3 magnetically equivalent and their average splitting (1.4 G) is

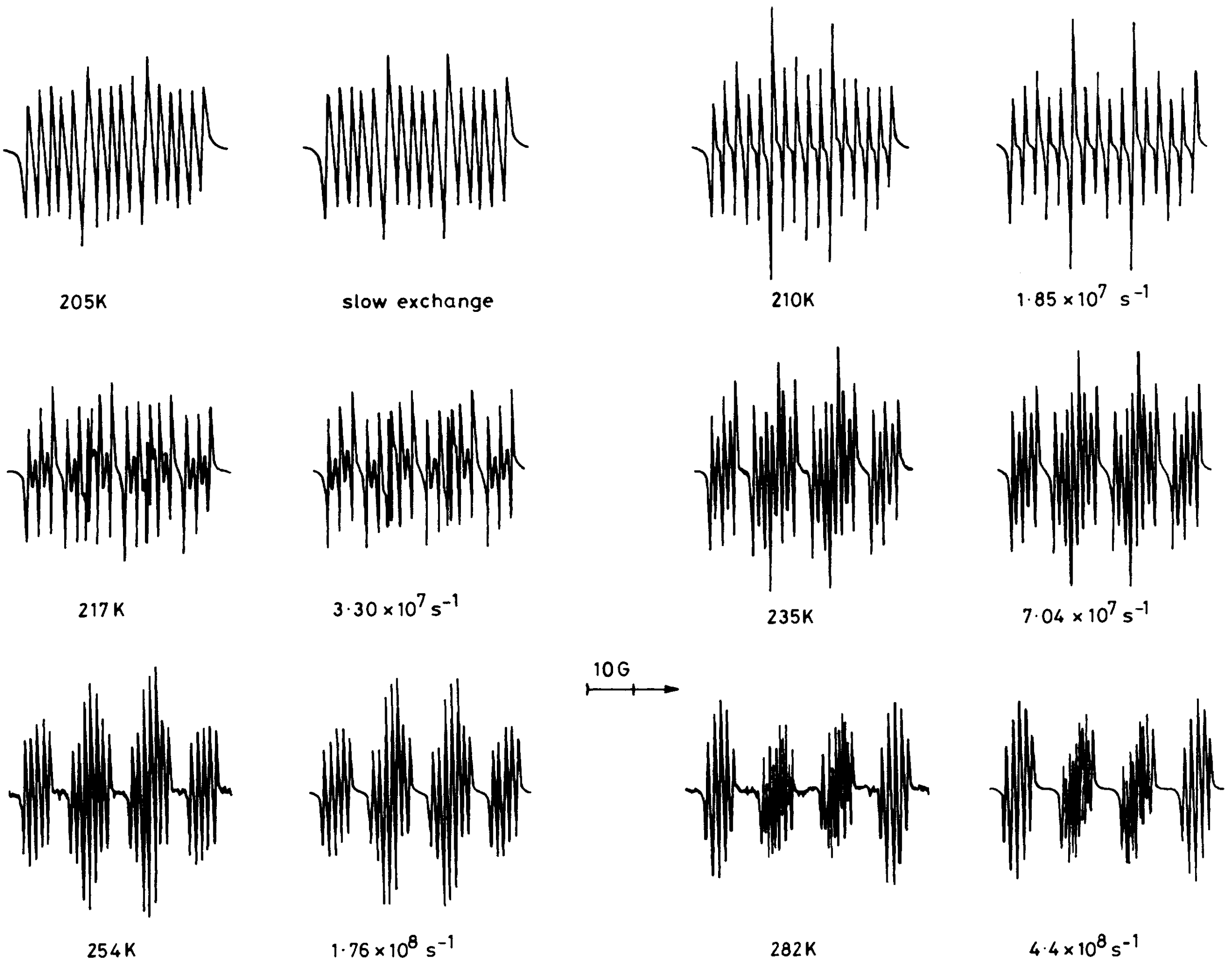

Figure 3. E.s.r. spectra of the spin-labelled phosphorane (11; R = Me) in cyclopropane. The temperatures are given below the observed spectra and the values k_{vi} are given beneath the computer simulations

observed at 282 K. These lineshape changes were computer simulated by assuming that the apical nitrogen splitting increases linearly with temperature from 2.6 G at 205 K to 2.8 G at 282 K, while the equatorial nitrogen splitting (unresolved) remains constant at 0.01 G. The simulated spectra are shown alongside the experimental ones in Figure 3 and the temperature dependence of k_{vi} can be represented by equation (vii).

$$\log_{10}(k_{vi}/\mathrm{s}^{-1}; \mathrm{R} = \mathrm{Me}) = (12.7 \pm 0.3) - (21.8 \pm 1.5)/2.303RT\ \mathrm{kJ\ mol}^{-1} \quad \text{(vii)}$$

Similarly, SLPs were formed by addition of (1; R = Bu^t) to triethyl or trineopentyl phosphite and to 2-neopentoxy- or 2-t-butoxy-1,3,2-dioxaphospholan (all *ca.* 1M), and the e.s.r. spectroscopic parameters are included in Table 2 (see Figure 4). Lineshape effects due to exchange of apical and equatorial nitrogens were also detected for (11; R = Et), but these effects were apparent at temperatures *ca.* 60 K higher than observed for (11; R = Me). Thus, the spectrum of (11; R = Et) at 272 K was similar in appearance to that of (11; R = Me) at 210 K (see Figure 3). The adduct (11; R = Pe^{neo}) also undergoes nitrogen exchange more slowly than (11; R = Me) and the e.s.r. spectrum showed no evidence of interconversion of (11a and b) up to 265 K. With trineopentyl phosphite (1.1M) below *ca.* 200 K and above *ca.* 240 K, the spectrum of (1; R = Bu^t) was observed in addition to that of (11; R = Pe^{neo}), indicating that at low temperatures addition to this sterically hindered phosphite is relatively slow, whilst at high temperatures the addition is reversible under the experimental conditions. With the same concentration of trimethyl or triethyl phosphite, (1; R = Bu^t) was not detectable within the temperature range studied.

For (13; R = Bu^t or Pe^{neo}) apical–equatorial nitrogen exchange was more rapid than for the acyclic SLPs and was still rapid on the e.s.r. time scale at 210 K. Figure 4 shows the spectrum of (13; R = Bu^t) at 249 K; below *ca.* 190 K the addition of (1; R = Bu^t) was incomplete and spectra of both addendum and SLP adduct were observed.

The radical (11; R = Et) was also detected during photolysis of cyclopropane or ethylene solutions containing diethyl peroxide and the phosphinotriazene (14) [equations (viii) and (ix)], but the presumed intermediate phosphoranyl radical (15) could not be detected even at very low temperatures. Similarly, photolysis of diethyl peroxide in the presence of the phosphinotriazene (16) at *ca.* 220 K gave rise to a spectrum which we ascribe to the SLP (5), in which apical–equatorial nitrogen exchange is rapid on the e.s.r. time scale (see Table 2). However, when the temperature was reduced to *ca.* 180 K the spectrum of (5) was replaced by one which we assign [12,17] to the triazenophosphoranyl radical (17) [a(P) 931.5, a(1N) 26.7 G, g 2.0020 at 163 K in cyclopropane]. This indicates that ethoxyl radicals add to (16) to form (17) which subsequently cyclises to give

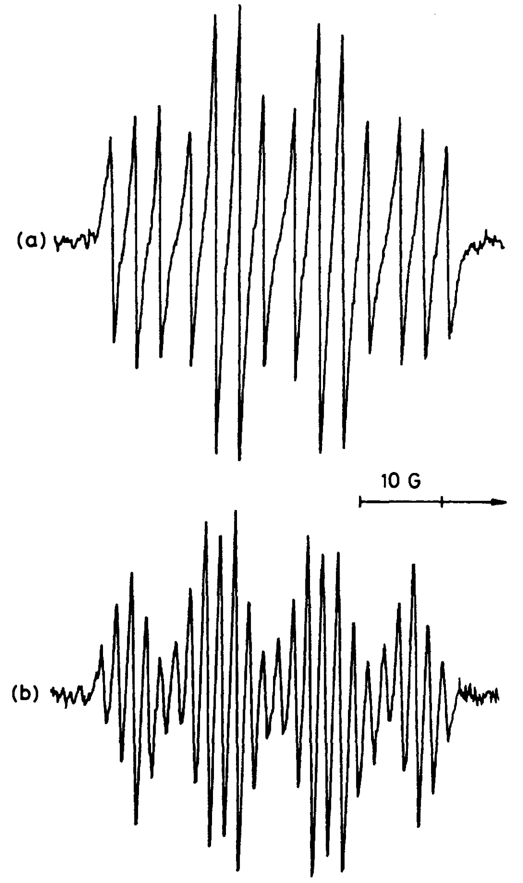

Figure 4. E.s.r. spectra of spin-labelled phosphoranes in cyclopropane at 249 K: (a) (11; R = Et), (b) (13; R = Bu^t)

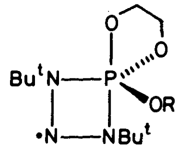

(13)

$$\mathrm{EtOOEt} \xrightarrow{h\nu} 2\mathrm{EtO}\bullet \qquad \text{(viii)}$$

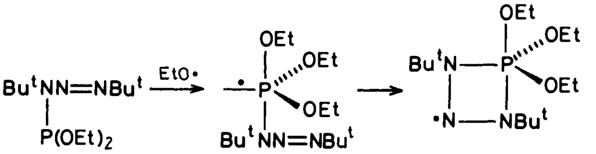

(ix)

(14) (15)

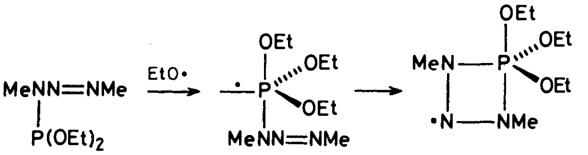

(x)

(16) (17) (5)

(5) [equation (x)]. The e.s.r. spectrum of the tetraethoxyphosphoranyl radical (EtO)$_4$P· was also apparent in the experiments with (14) and (16) and its intensity increased with the duration of photolysis.[*] This result implies that triethyl phosphite is also produced in the reaction of ethoxyl radicals with (14) and (16), probably because of α-scission of (15) and (17) to give the di-t-butyl- or dimethyl-triazenyl radical, respectively, although this route must represent a minor decay pathway for the phosphoranyl radicals.

As was mentioned above, photolysis of 1,3-dimethyltriazene and triethyl phosphite in cyclopropane–diethyl ether at 251 K also afforded a weak spectrum of (5). Neither (5) nor the phosphoranyl radical (17) could be detected when the experiment was repeated at 150 K, but this is not surprising since the linewidth for (17) is much greater than that for (5). Thus, it is not clear whether addition of (1; R = Bu^t or Me) to trialkyl phosphites yields directly the SLP or if an intermediate phosphoranyl radical [(15) or (17), respectively] is formed first.

Photolysis of (16) alone in cyclopropane at 170 K afforded a weak spectrum of the methyl radical and presumably $\mathrm{Me\dot{N}P(OEt)_2}$ was also formed, although this radical was not detected. Above *ca.* 210 K, the spectrum of the methyl radical was replaced by a weak complex spectrum, possibly from the SLP Me(EtO)$_2$P(NMe)$_2$N·. The same spectrum (stronger, but still not completely analysable) was observed during photolysis of a cyclopropane solution containing (16) and azomethane (a good source of Me·) at 230 K.

Discussion

Electronic Configuration of 1,3-*Dialkyltriazenyl Radicals.*—Assuming that the CNNNC skeleton is planar, the SOMO of a dialkyltriazenyl radical could be a σ- or a π-orbital and these molecular orbitals are illustrated in (18) and (19) for the (*E,E*)-configuration of the prototype radical $\overline{\mathrm{HN\dot{N}NH}}$. *Ab initio* MO calculations predict[2] that the σ-configuration (18) is the more stable, but only by 6.7 kJ mol^{-1}. The magnitudes of the nitrogen splittings for the dialkyltriazenyl radicals are clearly consistent with a σ SOMO, analogous to that shown in (18), and not with a π SOMO which has a node at the central nitrogen. When the magnetic field is directed parallel to the NNN plane and perpendicular to the two-fold axis, spin–orbit coupling would be expected to induce mixing of the σ ground state with an excited state in which the unpaired electron is promoted into the empty three-centre π* molecular orbital. If the resulting negative orbital contribution to the *g*-factor in this direction is dominant, it would lead to a g_{average} value less than free-spin (2.0023), as observed experimentally. Analogous effects are responsible for the low *g*-factors of $\dot{\mathrm{C}}\mathrm{O}_2^-$ and $\dot{\mathrm{N}}\mathrm{O}_2$, which are isoelectronic with the parent triazenyl radical.[19,20] A nitrogen-centred π-radical (19), with a full complement of 14 σ-electrons, would be expected to exhibit a *g*-factor significantly greater than 2.0023, as found for alkyl-substituted aminyl, hydrazyl, and triazyl radicals.

In valence bond terms, a dialkyltriazenyl σ-radical may be represented as a hybrid of canonical structures (20a—f), in which σ-electrons are shown above the formulae and π-electrons below. The contributions from (20c and f) should be small on account of the widely separated charges. Replace-

---

[*] For (EtO)$_4$P· at 230 K in ethylene, a(P) 885.7 G and g 2.0019. Apart from the doublet splitting due to ^{31}P, a further (previously unreported) partially resolved splitting into $\geqslant 7$ lines spaced by 0.18 G can be detected for this radical at 233 K.[18] We assign this splitting to the eight methylene protons of the four ethoxy-groups, which would be rendered equivalent on the e.s.r. time scale by their rapid exchange at this temperature.[12]

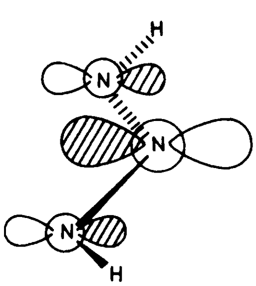

(18)

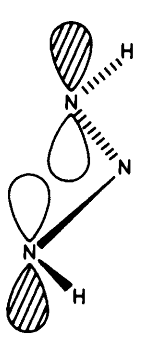

(19)

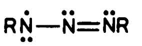
$\mathrm{R\underset{\cdot\cdot}{\dot{N}}-\ddot{N}{=}\ddot{N}R}$

(20a)

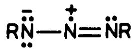
$\mathrm{R\underset{\cdot\cdot}{\overset{-}{\ddot{N}}}-\overset{+}{\dot{N}}{=}\ddot{N}R}$

(20b)

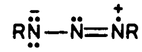
$\mathrm{R\underset{\cdot\cdot}{\overset{-}{\ddot{N}}}-\ddot{N}{=}\overset{+}{\dot{N}}R}$

(20c)

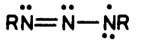
$\mathrm{R\ddot{N}{=}\ddot{N}-\underset{\cdot\cdot}{\dot{N}}R}$

(20d)

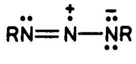
$\mathrm{R\ddot{N}{=}\overset{+}{\dot{N}}-\underset{\cdot\cdot}{\overset{-}{\ddot{N}}}R}$

(20e)

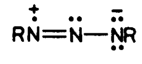
$\mathrm{R\overset{+}{\dot{N}}{=}\ddot{N}-\underset{\cdot\cdot}{\overset{-}{\ddot{N}}}R}$

(20f)

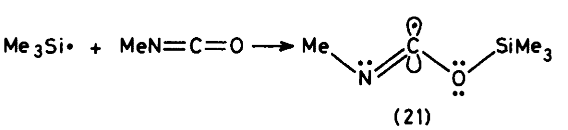
$$\mathrm{Me_3Si\cdot + MeN{=}C{=}O \longrightarrow Me\ddot{N}{=}\dot{C}{-}\ddot{O}{-}SiMe_3} \qquad \text{(xi)}$$

(21)

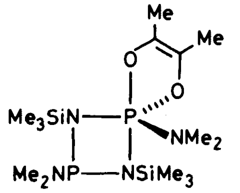

(22)

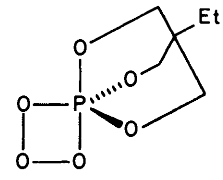

(23)

ment of one or both *N*-alkyl groups by trialkylsilyl groups, which are known to stabilise a negative charge on an attached nitrogen,[21] would be expected to result in increased contribution from (20b and e) and hence in increased spin-population on the central nitrogen and in the value of $a(\mathrm{N}^2)$, as observed. A similar rationalisation may be given for the large value of $a(\mathrm{N})$ in $\dot{\mathrm{N}}\mathrm{O}_2$, in which the RN groups in (20) are replaced by the more electronegative oxygen atoms. In molecular orbital terms, the σ SOMO is anti-bonding between the central nitrogen and the terminal groups, and hence an increase in the effective electronegativity of the latter will cause a shift of spin-population to the central atom. From Table 1 it is also evident that the *g*-factor decreases with successive replacements of alkyl by trialkylsilyl groups in (1). This may be attributed to the ability of $\mathrm{R_3Si}$ substituents to reduce the ($\sigma^* \longrightarrow \pi^*$) promotion energy as a consequence of the σ-donor–π-acceptor properties of the silicon ligand.[22]

The imidoyl radical (21) is isoelectronic with the triazenyl radical (2) and these species may be generated by the related addition reactions of $\mathrm{Me_3Si\cdot}$ with $\mathrm{MeN{=}C{=}O}$ [equation (xi)] and with $\mathrm{MeN{=}\overset{+}{N}{=}\overset{-}{N}}$ [equation (iv)], respectively. Radical (21) is also believed[23] to adopt a W configuration, as shown, and is a σ-radical in which the unpaired electron is primarily associated with the central carbon, as a result of the much lower electronegativity of carbon compared with that of nitrogen or oxygen.

The magnitudes of $a(2\mathrm{H})$ for (1; R = $\mathrm{Pr^i}$) and $a(6\mathrm{H})$ for (1; R = Me) are similar and, considering the pronounced dependence of $a(\mathrm{H})$ on dihedral angle expected on the basis of the INDO calculations [see (10)], do not indicate any marked conformational preference about the C–N bonds in the former radical.

Spin-labelled Phosphoranes.—Pentaco-ordinate phosphoranes in which the phosphorus atom is part of a four- or five-membered ring system are particularly stable and many examples of such species are known, for example (22)[24] and (23).[25]

The e.s.r. parameters indicate that the unpaired electron in the SLPs (5), (11), and (13) is centred mainly on N^2 and occupies a π-type orbital; the phosphorus and three nitrogen atoms are probably co-planar in the most stable conformation of the four-membered ring. The e.s.r. spectrum of the acyclic triazyl radical $\mathrm{(Me_3Si)_2N\dot{N}N(SiMe_3)_2}$ has been reported previously[26] and shows $a(1\mathrm{N})$ 14.6 and $a(2\mathrm{N})$ 1.5 G. The $^{31}\mathrm{P}$-splittings for the SLPs increase rapidly with increasing temperature, probably as a result of Boltzmann population of excited ring-vibrational states in which the phosphorus atom is out of the plane defined by the three nitrogen atoms. In such excited states, the P-3*s* orbital will contribute to the SOMO, giving rise to a positive component in $a(\mathrm{P})$. The implication is that $a(\mathrm{P})$ is positive at all temperatures investigated. Although the SLPs and the phosphoranes (22) and (23) are shown as having regular trigonal–bipyramidal co-ordination at phosphorus, this is only for convenience and there will undoubtedly be some distortion towards square-pyramidal geometry, especially for the species which contain both four- and five-membered ring systems.[27]

Since the SLPs are π-radicals and the triazenyl radicals are σ-radicals, we might expect a ' symmetry ' barrier to the direct formation of the former by addition of the latter to $\mathrm{(RO)_3P}$. Similarly, cyclisation of a σ triazenophosphoranyl radical [*e.g.* (17)] would be symmetry ' forbidden ' if a rigidly planar four-membered ring is formed. However, these symmetry constraints do not appear to result in substantial barriers to the addition or cyclisation reactions, possibly because non-planar conformations of the ring are thermally populated at the temperatures involved (see above).

Apical–equatorial ligand exchange in diamagnetic pentaco-ordinate phosphoranes is a well documented phenomenon and has been studied extensively both theoretically and experimentally, often by dynamic n.m.r. methods.[27,28] The exchange is generally thought to proceed by the Berry pseudorotation mechanism,[29] shown in equation (xii) for pentafluorophosphorane, and to involve a square-pyramidal transition state. The pivotal ligand F^1 is equatorial before and after exchange and is apical in the square-pyramidal structure. It seems likely that the Berry mechanism is also responsible for apical–equatorial nitrogen ligand exchange in the SLPs. More bulky basal ligands would be expected to destabilise the square-pyramidal transition state relative to the trigonal-bipyramidal ground state and hence we can understand why both (5) and (11; R = Me) undergo nitrogen exchange more readily than (11; R = Et or $\mathrm{Pe^{neo}}$). The presence of both four- and five-membered rings in (13) would be expected to lead to ground state geometries which are displaced significantly along the Berry distortion co-ordinate from regular trigonal-bipyramidal towards square-pyramidal, and thus to result in a lower barrier to nitrogen exchange for these spirocyclic SLPs.[27]

Since the e.s.r. time scale is *ca.* 10^6—10^7 times faster than the n.m.r. time scale, much more rapid exchange processes are amenable to study by dynamic e.s.r. spectroscopy. Thus, exchange in $\mathrm{PF_5}$ itself [equation (xii)] has not yet been slowed

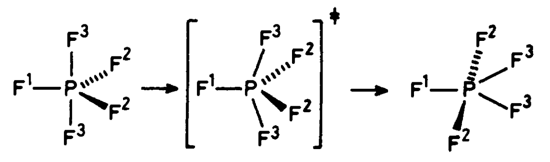

(xii)

on the n.m.r. time scale down to 83 K.[27,30] Calculations of the barrier have given values between 6 and 20 kJ mol^{-1},[27] at the upper end close to the value found experimentally for the barrier to apical–equatorial nitrogen exchange in (11; R = Me). E.s.r. spectroscopy can be used to monitor exchange processes for SLPs that would not be easily detectable for the analogous diamagnetic phosphoranes using n.m.r. spectroscopic techniques, which are usually employed to measure barriers in the range 40—120 kJ mol^{-1}.[27]

Experimental

The techniques used for the generation and detection by e.s.r. spectroscopy of transient free radicals in solution have been described previously.[6,31] Computer simulation of lineshape effects resulting from ligand exchange in the SLPs was accomplished using the program ESREXN written by Dr. J. Heinzer and obtained from Q.C.P.E. (program no. 209).

Materials.—1,3-*Dimethyltriazene*. Methyl azide[32] (15.0 g, 0.26 mol) was condensed into a flask containing methyllithium in diethyl ether (1.4M, 130 ml, 0.18 mol) cooled in a solid CO_2–ethanol bath. Pentane (100 ml) was then added and the mixture was stirred and allowed to warm to room temperature. After stirring for a further 2 h, a straw-yellow solution remained. The flask was cooled in an ice–salt bath and hydrolysed with an aqueous solution containing 10% w/v of both NH_4Cl and NH_4OH (50 ml). The organic phase was separated and the aqueous phase extracted with pentane (100 ml). The combined organic fractions were then dried (Na_2SO_4) and carefully fractionated to yield the product (37%), b.p. 46—47 °C at 100 Torr [lit.,[33] 92 °C (decomp.) at atmospheric pressure]. The ^1H n.m.r. spectrum (60 MHz, C_6D_6, 37 °C) showed broad singlets at δ 2.77 and 3.43 as reported in ref. 34. The mass spectrum (at 70 eV) showed m/e 73 (M^+, 18%) and 43 (base peak).

To remove traces of solvent,[33] the dimethyltriazene was further purified by preparative g.l.c. at 70 °C using a 9 mm × 2.1 m glass column packed with 15% PEG 20 M on AWDMCS Diatomite C.

1,3-Bis(trideuteriomethyl)triazene was prepared by the method used for the protio-compound by Lunazzi *et al.*[34] CD_3N_3 was prepared[32] from $(CD_3O)_2SO_2$ (Aldrich) and CD_3MgI from CD_3I (Aldrich). The triazene was purified by preparative g.l.c. as described for the protio-compound. The mass spectrum (at 70 eV) showed m/e 79 (M^+, 13%) and 46 (base peak).

1,3-*Di-isopropyltriazene*. Isopropylmagnesium bromide in diethyl ether (1.05M, 115 ml, 0.12 mol) was added dropwise with stirring to isopropyl azide[35] (10.0 g, 0.12 mol) in diethyl ether (50 ml) cooled in a solid CO_2–ethanol bath. The mixture was allowed to warm to room temperature, stirred for a further 2 h, and then hydrolysed by addition of aqueous 10% w/v NH_4Cl + 10% w/v NH_4OH (50 ml). The organic phase was washed with water (100 ml), dried (K_2CO_3), and carefully fractionated to give the *product* (20%), b.p. 53—54 °C at 15 Torr (Found: C, 56.2; H, 11.8; N, 32.4. $C_6H_{15}N_3$ requires C, 55.8; H, 11.7; N, 32.5%). The ^1H n.m.r. spectrum (60 MHz, C_6D_6, 37 °C) showed δ 0.99 [d, J 7.1 Hz, $CH(CH_3)_2$] and 3.74 [septet, J 7.1 Hz, $CH(CH_3)_2$] from two magnetically equivalent[34] isopropyl groups. The mass spectrum (at 70 eV) showed m/e 129 (M^+, 2%) and 43 (base peak).

1,3-*Di-t-butyltriazene*. t-Butyl-lithium in pentane (1.0M, 70 ml, 0.070 mol) was added dropwise to t-butyl azide[36] (6.0 g, 0.061 mol) in diethyl ether (50 ml) while stirring and cooling in a solid CO_2–ethanol bath. The mixture was allowed to warm to room temperature and then stirred for a further 2 h. The solution was cooled in an ice–salt bath, hydrolysed with aqueous 10% w/v NH_4Cl + 10% w/v NH_4OH (50 ml), and the organic phase was separated. The aqueous phase was extracted with diethyl ether (2 × 100 ml) and the combined organic fractions were dried (Na_2SO_4) and fractionally distilled to give the *product* (70%), b.p. 72—74 °C at 50 Torr (Found: C, 61.3; H, 12.0; N, 26.9. $C_8H_{19}N_3$ requires C, 61.1; H, 12.2; N 26.7%). The ^1H n.m.r. spectrum (60 MHz, C_6D_6, 37 °C) showed δ 1.2 (s) from magnetically equivalent[34] t-butyl groups. The mass spectrum (at 70 eV) showed m/e 157 (M^+, 0.5%) and 57 (base peak).

Phosphorus compounds. Trimethyl and triethyl phosphites were commercial products purified by distillation before use. Trineopentyl phosphite,[37] 2-t-butoxy-,[38] and 2-neopentoxy-1,3,2-dioxaphospholans[39] were prepared as described in the literature. The triazenophosphines were prepared under dry nitrogen as described below.

1-*Diethoxyphosphino*-1,3-*dimethyltriazene*. The lithium salt of dimethyltriazene was prepared as described above from methyl azide (10.3 g, 0.18 mol) and methyl-lithium in diethyl ether (1.5M, 107 ml, 0.16 mol). This solution was cooled in an ice-bath and diethyl chlorophosphite (28.9 g, 0.18 mol) in diethyl ether (50 ml) was added dropwise with stirring. The mixture was stirred at room temperature for 12 h, the precipitated lithium chloride was removed by filtration, the solvent removed under reduced pressure, and the residue was distilled to give the *product* (74%), b.p. 56—57 °C at 2 Torr (Found: C, 37.2; H, 8.2; N, 22.1; P, 16.1. $C_6H_{16}N_3O_2P$ requires C, 37.3; H, 8.3; N, 21.8; P, 16.0%). The n.m.r. spectra (in C_6D_6) showed δ_H 1.35 (t, J 6.7 Hz, CH_3CH_2O), 2.98 (d, J 1.6 Hz, $PNCH_3$), 3.60 (s, $N{=}NCH_3$), and 3.95 (d of q, J_{H-H} 6.7, J_{P-H} 8.6 Hz, $POCH_2CH_3$); δ_P (proton-decoupled) 142.1 p.p.m. downfield from external 85% aqueous H_3PO_4.

1-*Diethoxyphosphino*-1,3-*di-t-butyltriazene* was prepared in 46% yield by a similar procedure starting from t-butyl azide (7.9 g, 0.080 mol) and t-butyl-lithium (0.080 mol) in pentane, b.p. 75—76 °C at 0.2 Torr (Found: C, 52.1; H, 10.0; N, 14.8; P, 11.4. $C_{12}H_{28}N_3O_2P$ requires C, 52.0; H, 10.2; N, 15.2; P, 11.2%). The ^1H n.m.r. spectrum in C_6D_6 showed δ 1.16 (t, J 6.7 Hz, CH_3CH_2O), 1.25 (s, $PNC_4H_9{}^t$), 1.60 (s, $N{=}NC_4H_9{}^t$), and 3.88 (d of q, J_{H-H} 6.7, J_{P-H} 8.6 Hz, $POCH_2CH_3$).

Acknowledgements

We are very grateful to Drs. T. Clark and J. E. Parkin for help in running the MINDO/3-UHF computer program and we acknowledge financial support from the S.E.R.C.

References

1 M. C. R. Symons, 'Chemical and Biochemical Aspects of Electron Spin Resonance Spectroscopy,' Van Nostrand-Reinhold, London, 1978, pp. 62—64.
2 N. C. Baird and K. F. Taylor, *Can. J. Chem.*, 1980, **58**, 733.
3 F. Bernardi, M. Guerra, L. Lunazzi, G. Panciera, and G. Placucci, *J. Am. Chem. Soc.*, 1978, **100**, 1607.
4 J. C. Brand and B. P. Roberts, *J. Chem. Soc., Chem. Commun.*, 1981, 748.

5 J. C. Brand and B. P. Roberts, *J. Chem. Soc., Chem. Commun.*, 1981, 1107.

6 J. A. Baban and B. P. Roberts, *J. Chem. Soc., Perkin Trans. 2*, 1981, 161.

7 H. Kiefer and T. G. Traylor, *Tetrahedron Lett.*, 1966, 6163.

8 B. P. Roberts and J. N. Winter, *J. Chem. Soc., Perkin Trans. 2*, 1979, 1353.

9 J. C. Brand and B. P. Roberts, unpublished work.

10 H. Paul and H. Fischer, *Helv. Chim. Acta*, 1973, **56**, 1575.

11 J. C. Scaiano and G. G. Wubbels, *J. Am. Chem. Soc.*, 1981, **103**, 640.

12 B. P. Roberts, *Adv. Free Radical Chem.*, 1980, **6**, 225; J. R. M. Giles and B. P. Roberts, *J. Chem. Soc., Perkin Trans. 2*, 1981, 1211.

13 P. Bischof, *J. Am. Chem. Soc.*, 1976, **98**, 6844.

14 W. A. Lathan, L. Radom, P. C. Hariharan, W. J. Hehre, and J. A. Pople, *Top. Curr. Chem.*, 1973, **40**, 1.

15 A. R. Gregory, *J. Chem. Phys.*, 1974, **60**, 3713.

16 E. L. Muetterties, W. Mahler, and R. Schmutzler, *Inorg. Chem.*, 1963, **2**, 613; R. Hoffmann, J. M. Howell, and E. L. Muetterties, *J. Am. Chem. Soc.*, 1972, **94**, 3047.

17 J. A. Baban and B. P. Roberts, *J. Chem. Soc., Perkin Trans. 2*, 1980, 876.

18 A. J. Price and B. P. Roberts, unpublished work.

19 D. W. Ovenall and D. H. Whiffen, *Mol. Phys.*, 1961, **4**, 135.

20 P. W. Atkins, N. Keen, and M. C. R. Symons, *J. Chem. Soc.*, 1962, 2873.

21 K. J. Shea, R. Gobeille, J. Bramblett, and E. Thompson, *J. Am. Chem. Soc.*, 1978, **100**, 1611; L. Noodlemann and N. L. Paddock, *Inorg. Chem.*, 1979, **18**, 354 and references contained in these papers.

22 J. C. Brand, M. D. Cook, A. J. Price, and B. P. Roberts, *J. Chem. Soc., Chem. Commun.*, 1982, 151.

23 J. A. Baban, M. D. Cook, and B. P. Roberts, *J. Chem. Soc., Perkin Trans. 2*, 1982, 1247.

24 W. Zeiss, *Angew. Chem, Int. Ed. Engl.*, 1976, **15**, 555.

25 M. E. Brennan, *Chem. Commun.*, 1970, 956; L. M. Stephenson and D. E. McClure, *J. Am. Chem. Soc.*, 1973, **95**, 3074.

26 R. West and B. Bichlmeir, *J. Am. Chem. Soc.*, 1973, **95**, 7897

27 R. R. Holmes, *Acc. Chem. Res.*, 1979, **12**, 257.

28 R. Luckenbach, ' Dynamic Stereochemistry of Pentaco-ordinated Phosphorus and Related Elements,' Thieme, Stuttgart, 1973.

29 R. S. Berry, *J. Chem. Phys.*, 1960, **32**, 933.

30 R. P. Carter, jun., and R. R. Holmes, *Inorg. Chem.*, 1965, **4**, 738; E. L. Muetterties, *Acc. Chem. Res.*, 1970, **3**, 266.

31 P. M. Blum and B. P. Roberts, *J. Chem. Soc., Perkin Trans. 2*, 1978, 1313.

32 J. Bragin, S. Chan, E. Mazzola, and H. Goldwhite, *J. Phys. Chem.*, 1973, **77**, 1506.

33 O. Dimroth, *Ber.*, 1906, **39**, 3905.

34 L. Lunazzi, G. Panciera, and M. Guerra, *J. Chem. Soc., Perkin Trans. 2*, 1980, 52.

35 E. Lieber, T. S. Chao, and C. N. R. Rao, *J. Org. Chem.*, 1957, **22**, 654.

36 J. A. Miller, *Tetrahedron Lett.*, 1975, 2959.

37 H. R. Hudson, R. G. Rees, and J. E. Weekes, *J. Chem. Soc., Perkin Trans. 1*, 1974, 982.

38 R. Burgada, H. Germa, M. Willson, and F. Mathis, *Tetrahedron*, 1971, **27**, 5833; B. P. Roberts and K. Singh, *J. Chem. Soc., Perkin Trans. 2*, 1980, 1549.

39 J. W. Cooper, M. J. Parrott, and B. P. Roberts, *J. Chem. Soc., Perkin Trans. 2*, 1977, 730.

Received 5th *May* 1982; *Paper* 2/734